上の尿量を確保するように努める）を確保する。もし患者が十分な水分摂取ができ，十分な尿量が得られている場合は，必ずしも点滴静注を行う必要はない。もし基準の尿量が得られない，もしくは体重増加をきたした場合は，利尿薬を投与する。また，シスプラチン投与により低マグネシウム血症が起こり，加えて低マグネシウム血症がシスプラチンによる腎毒性を増悪させるため[3]，輸液にマグネシウム製剤を加えることも重要である。当院では入院で化学療法を行っているが，day 2 以降に飲水を取れれば輸液投与は不要であることから，外来投与が可能なレジメンである。

2．TC 療法

TC 療法（パクリタキセル＋カルボプラチン）は卵巣癌で用いられる標準療法である[4]。パクリタキセル175 mg/m²（3 時間で静注），カルボプラチン AUC 6 を 3 週ごとに投与するレジメンである。当院では初回から外来投与で行っているが，今回は入院での投与を想定し，**表 2** にクリニカルパスの例を示す。

クリニカルパス作成において重要となるポイントは，パクリタキセルによる過敏性反応である。パクリタキセルの溶解剤である polyoxethylated castor oil vehicle（クレモフォール EL）による反応と考えられている。初期の臨床試験ではパクリタキセルによる過敏性反応が高頻度に起こったため，アレルギー予防のためにパクリタキセル投与の12時間前，6 時間前にデキサメタゾン20 mg を経口投与していた。ところが近年，short premedication といわれる，パクリタキセル投与の30分前にリン酸デキサメタゾン20 mg，ジフェンヒドラミン50 mg，シメチジン300 mg もしくはラニチジン50 mg を静注することにより，過敏性反応の発現を予防することができることが示された[5]。過敏

表 1　AP 療法クリニカルパスの一例

クリニカルパス名　AP療法（子宮体癌）　コース目
患者氏名　様　ID　担当医：

適応基準
1) 子宮体癌Ⅲ期術後またはⅣ期
2) 75歳以下
3) PSが0から3
4) 好中球1,000/μL
5) 血小板10万以上
6) クレアチニン2.0 mg/dL 未満

年月日		／　／		／
病日		入院		day 1
達成目標				嘔気・嘔吐がGrade 1 以下である 尿量が1,500 mL 以上確保されている
指示	薬剤			9：00　①生食　1,000 mL　3時間 12：00　②生食50 mL リン酸デキサメタゾン20 mg グラニセトロン1A(1 mg/3 mg)15分 12：15　③アドリアマイシン　mg 生食50 mL　15分 12：30　④シスプラチン　mg 生食250 mL　60分 13：30　⑤生食500 mL　60分 15：00　⑥D-マンニトール200 mL　15分 15：30　⑦生食500 mL+硫酸マグネシウム液1A60分 18：30　終了
		悪心・嘔吐時（①から④の順番に） ①メトクロプラミド　5 mg　4錠（1日5回まで，経口不能時②へ） ②ドンペリドン坐剤60 mg　1個 ③生食　50 mL＋メトクロプラミド　40 mg　4 A/15分（1日4回まで） ④アルプラゾラム0.4 mg　1錠（1日3回まで）		
	尿量・体重測定指示	1日1回測定（入院時）		①　尿量測定：9時から19時 19時尿量1,000 mL 以下のとき ②　体重測定：10時，18時 18時体重がday 1(10時)の値より2 kg 以上増加したとき ①あるいは②の場合，フロセミド10 mg ワンショット静注
	その他指示	有・無		有・無
処置		尿道準備		サーフロー挿入 ヘパロック
検査		血算・生化		
活動安静度		制限なし		制限なし
栄養		栄養指導（入院時） NST 依頼票提出		
排泄				尿測
清潔		入浴可		入浴可
指導・説明		入院治療計画書 入院オリエンテーション（看護師） 治療オリエンテーション（医師）		シスプラチン終了時までに飲水1,000 mL を終了しておく
観察	体重	kg		10時　kg 19時　kg
	尿量			10時～19時　mL 1日尿量　mL
	体温（℃）			
	脈拍（回/分）			
	血圧（mmHg）			
	食事摂取量			
	排便			
	悪心			
	嘔吐			
	食欲不振			
	便秘			
	倦怠感			
	血管外漏出			
経過記録				
予測される看護診断				
バリアンス				
担当看護師名				

担当看護師：　　医療者用

	退院基準
7）ALT/AST　100未満 8）合併症を有する場合，経口薬投与で症状が安定している。	day 4 にコップ 1 杯の水を飲むことができる

day 2	day 3	day 4
嘔気・嘔吐が Grade 1 以下である 尿量が1,500 mL 以上確保されている 水分摂れていれば下記点滴不要，退院可	嘔気・嘔吐が Grade 1 以下である 水分摂れていれば下記点滴不要， 退院可	コップ 1 杯の水を飲むことができる
9：00　①生食50 mL リン酸デキサメタゾン16 mg 15分 9：15　②生食　1,500 mL +硫酸マグネシウム液　1 A 6時間	9：00　①生食50 mL リン酸デキサメタゾン 16mg 15分 9：15　②生食1,500 mL +硫酸マグネシウム液 1 A　6時間	
便秘時 酸化マグネシウム（カマ，マグミット），センノシド，ピコスルファートナトリウム内服可 GE，レシカルボン坐薬使用可 （各薬剤の投与量，タイミングは調節可） 発熱時（38.0℃以上） ①アセトアミノフェン（200）2 錠内服	不眠時 ゾピクロン　7.5 mg　1 錠 （追加 1 錠まで可） 退院時の発熱時処方（38.0℃以上） ①アセトアミノフェン（200）6 錠分 3 内服 ②塩酸シプロフロキサシン（200）6 錠分 3 内服 7 日間継続	
尿量測定（1日量のみ）1,500 mL 以下のとき フロセミド　10 mg　ワンショット静注	尿量測定（1 日量のみ）1,500 mL 以下のとき フロセミド10 mg　ワンショット静注	
有・無	有・無	有・無
ヘパロック （点滴ない場合，サーフロー抜去）	終了後サーフロー抜去	
制限なし	制限なし	
栄養指導（初回のみ）		
尿測	尿測	
入浴可	入浴可	
	退院時オリエンテーション 退院時処方確認 退院療養計画書	
19時　kg		
10時～19時　mL 1 日尿量　mL	1 日尿量　mL	

＊ grade は NCI CTC AE ver 3.0にて評価すること。
国立がんセンター中央病院　16A 病棟　2007年 3 月改訂

9

表２　TC 療法クリニカルパスの一例

クリニカルパス名：TC 療法　（一泊診療）　　（　　）コース目
患者 ID：　　患者氏名：　　担当医：　　担当看護師：

在院日数：２日

適応基準　１）原発不明癌　２）卵巣癌術後　３）卵巣癌再発後　４）婦人科系悪性腫瘍　５）泌尿器系悪性腫瘍　６）呼吸器系悪性腫瘍　７）好中球数≧1,500/mm³　８）血小板数≧75,000/mm³　９）GOT/GPT 100 Iuml 未満　10）PS 0～3

年月日		（　／　）	（　　／　　）	（　／　）
病日		入院前	Day１（入院日）	Day２（退院日）
達成目標			悪心・嘔吐が grade１以下である。コップ1杯の水を摂取可能である	
指示	薬剤		①生食50 mL リン酸デキサメタゾン20 mg ラニチジン　50 mg/２mL　15分 ②生食50 mL クロルフェニラミンマレイン酸塩　10 mg　15分 ③５％ブドウ糖　250 mL パクリタキセル＿＿＿＿＿mg　180分 ④生食50 mL グラニセトロン　１mg・３mg　15分 ⑤生食250 mL カルボプラチン＿＿＿＿＿mg　60分 ⑥生食50 mL　15分	デキサメタゾン0.5 mg 16錠分２（朝・昼食後） ラニチジン150 mg 錠 ２錠分２(朝食後・眠前) 38℃発熱時 塩酸シプロフロキサシン（200）６錠分３で７日間内服開始 アセトアミノフェン（200）１回２錠１日３回まで
			不眠時：ゾピクロン7.5 mg１錠（追加１錠まで可） 発熱（38℃以上）時：①アセトアミノフェン（200mg）２錠内服 ②アセトアミノフェン内服でも解熱なければ Drcall 悪心・嘔吐時：①メトクロプラミド５mg４錠内服（１日５回まで，経口不能時③へ） ②生食 50 mL＋メトクロプラミド40 mg　４A /15分（１日４回まで） ③アルプラゾラム0.4 mg（１日３回まで） 便秘時：酸化マグネシウム（マグミット），センノシド，ピコスルファートナトリウム当日排便なければ内服可。 GE，レシカルボン坐薬使用可	
	その他		有・無	有・無
処置			サーフロー挿入。終了時サーフロー抜針。 （１コース目のみヘパロック） パクリタキセル専用ルートを使用 １コース目のみ ECG モニター装着（パクリタキセル中のみ） （アラーム設定；不整脈，HR60未満160以上 Drcall） バイタル測定パクリタキセル前・中・後	
検査		採血 CT（３・５・７コース目の前）		
活動・安静度			制限なし	制限なし
栄養			常食（本人の希望にて変更可）	
排泄			尿測不要	尿測不要
清潔			入浴可	入浴可
指導・説明			入院治療計画書　退院診療計画書 入院オリエンテーション（看護師）　退院オリエンテーション 治療オリエンテーション（医師）　①退院処方 ②次回入院日 ③次回外来時 ④CT，採血の有無	塩酸シプロフロキサシンを３日間内服しても解熱しない場合，悪寒がある，呼吸苦がある場合は病院に連絡するよう説明
観察			タキソール投与前　投与中　投与後	
	体温（℃）			
	脈拍(回/分)			
	血圧(mmHg)			
	悪心			
	嘔吐			
	静脈炎			
	アレルギー反応			
経過記録				
予測される看護診断				
バリアンス				
担当看護師サイン				

国立がんセンター中央病院

医療者用

退院基準：コップ1杯の水を摂取可能		
(　/　)	(　/　)	(　/　)
Day 3	Day 4	Day 5
デキサメタゾン0.5 mg 12錠分2 (朝・昼食後) ラニチジン 150 mg 2錠分2 (朝食後・眠前)	デキサメタゾン0.5 mg 8錠分2 (朝・昼食後) ラニチジン 150 mg 2錠分2 (朝食後・眠前)	デキサメタゾン0.5 mg 4錠分2 (朝・昼食後) ラニチジン 150 mg 2錠分2 (朝食後・眠前)

乳腺腫瘍内科（16A 病棟）　2007年3月改訂

NCI-CTC AE ver.3.0による観察項目

有害事象	Grade 0	Grade 1	Grade 2	Grade 3	Grade 4
悪心	なし	摂食習慣に影響のない食欲低下	顕著な体重減少，脱水または栄養失調を伴わない経口摂取量の減少；<24時間の静脈内輸液を要する	カロリーや水分の経口摂取が不十分；≥24時間の静脈内輸液／経管栄養／TPNを要する	生命を脅かす
嘔吐	なし	24時間に1エピソードの嘔吐	24時間に2-5エピソードの嘔吐；<24時間の静脈内輸液を要する	24時間に≥6エピソードの嘔吐；≥24時間の静脈内輸液またはTPNを要する	生命を脅かす
静脈炎	なし		あり		
アレルギー反応	なし	一過性の潮紅あるいは皮疹；<38℃の薬剤熱	皮疹：潮紅：蕁麻疹；呼吸困難<38℃の薬剤熱	蕁麻疹の有無によらず症状のある気管支痙攣：非経口的治療を要する；アレルギーによる浮腫／血管性浮腫；血圧低下	アナフィラキシー

9

性反応への対応として，パクリタキセル投与前にshort-premedicationを行い，バイタル測定を行う。初回投与では投与中に心電図モニターを装着する。もし過敏性反応が起こった場合はバリアンスとなり，過敏性反応に対する治療を行うとともに，症例に応じてパクリタキセルの投与方法の変更，投与中止を行う。

3．悪心嘔吐に対する対策

化学療法に伴う副作用として，いずれのレジメンにおいても問題となるのは，悪心嘔吐である。ASCO（American Society of Clinical Oncology）ガイドライン，MASCC（Multinational Association of Supportive Care in Cancer）のコンセンサス会議により抗がん剤の催吐性リスク分類が提唱されており[6,7]，それによるとシスプラチンは高リスク，ドキソルビシン，カルボプラチンは中間リスクに分類されており，十分な悪心嘔吐対策が必要である。

化学療法投与開始から24時間以内の急性嘔吐に対しては，5-HT_3受容体拮抗薬と副腎皮質ステロイドの併用が勧められる[7]。ASCOガイドラインではaprepitantを含めた3剤併用を勧めているが，aprepitantは日本ではまだ承認されていない。上記薬剤で無効であれば，メトクロプロミド，アルプラゾラムの追加を行う。化学療法投与開始から24時間以降の遅発性嘔吐に対しては副腎皮質ステロイドの投与が確立しており，それにて効果がなければメトクロプロミド，アルプラゾラムの追加投与を行う。5-HT_3受容体拮抗薬の有効性は定かでなく，投与は勧められない。処方例を以下に示す。詳しくはASCOガイドラインを参照されたい。

＜シスプラチン（high emetic risk）投与時＞
day 1　　・カイトリル®（グラニセトロン）1 mg静

注もしくは2 mg経口
・デカドロン®24 mg（aprepitant併用時は16 mg）静注もしくは経口

day 2–3　・デカドロン®20 mg（aprepitant併用時は10 mg）静注または経口

※デカドロン®4 mg中にはデキサメタゾンとして3.3 mgしか含有していないことに注意

悪心時　・プリンペラン®（メトクロプラミド）20 mg静注または経口
・ソラナックス®（アルプラゾラム）0.4 mg静注または経口

おわりに

婦人科癌で代表的に用いられるレジメンのクリニカルパスの例を示し，重要な事項についてそれぞれ説明した。各病院の実情に合わせ，かつエビデンスに基づいたクリニカルパスを作成し発展させていくことにより，より一層適正で良質な医療が提供されるものと思われる。

（原野　謙一，勝俣　範之）

◉ References

1) Randall ME, Filiaci VL, Muss H et al : Randomized phase Ⅲ trial of whole-abdominal irradiation versus doxorubicin and cisplatin chemotherapy in advanced endometrial carcinoma : a Gynecologic Oncology Group Study. *J Clin Oncol* **24**(1) : 36–44, 2006

2) Launay-Vacher V, Rey JB, Isnard-Bagnis C et al : Prevention of cisplatin nephrotoxicity : state of the art and recommendations from the European Society of Clinical Pharmacy Special Interest Group on Cancer Care. *Cancer Chemother Pharmacol* **61**(6) : 903–909, 2008

3) Lajer H, Kristensen M, Hansen HH et al : Magnesium depletion

enhances cisplatin-induced nephrotoxicity. *Cancer Chemother Pharmacol* **56**(5)：535-542, 2005
4) Ozols RF, Bundy BN, Greer BE et al：Phase Ⅲ trial of carboplatin and paclitaxel compared with cisplatin and paclitaxel in patients with optimally resected stage Ⅲ ovarian cancer：a Gynecologic Oncology Group study. *J Clin Oncol* **21**(17)：3194-3200, 2003
5) Bookman MA, Kloth DD, Kover PE, Smolinski S, Ozols RF：Short-course intravenous prophylaxis for paclitaxel-related hypersensitivity reactions. *Ann Oncol* **8**(6)：611-614, 1997
6) Grunberg SM, Osoba D, Hesketh PJ et al：Evaluation of new antiemetic agents and definition of antineoplastic agent emetogenicity-an update. *Support Care Cancer* **13**(2)：80-84, 2005
7) American Society of Clinical Oncology, Kris MG, Hesketh PJ et al：American Society of Clinical Oncology guideline for antiemetics in oncology：update 2006. *J Clin Oncol* **24**(18)：2932-2947, 2006

Available online at www.sciencedirect.com
ScienceDirect
Gynecologic Oncology 108 (2008) 627–631
Gynecologic Oncology
www.elsevier.com/locate/ygyno

A synthetic retinoid, TAC-101 (4-[3,5-bis (trimethylsilyl) benzamido] benzoic acid), plus cisplatin: Potential new therapy for ovarian clear cell adenocarcinoma

Sachiko Ezawa [a], Nao Suzuki [b], Shinji Ohie [c], Atsushi Higashiguchi [a], Fumihito Hosoi [c], Kenji Kitazato [d], Nobuyuki Susumu [a], Daisuke Aoki [a,*]

[a] *Department of Obstetrics and Gynecology, School of Medicine, Keio University, 35 Shinanomachi, Shinjuku-ku, Tokyo 160-8582, Japan*
[b] *Department of Obstetrics and Gynecology, St. Marianna University School of Medicine, Kanagawa, Japan*
[c] *Personalized Medicine Research Laboratory, Tokushima Research Center, TAIHO Pharmaceutical Co., Ltd., Japan*
[d] *Strategic R&D Planing Department, Taiho Pharmaceutical Co., Ltd., Tokyo, Japan*

Received 28 May 2007

Abstract

Objective. A novel retinoid, TAC-101 (4-[3,5-bis (trimethylsilyl) benzamido] benzoic acid), induces apoptosis of ovarian clear cell adenocarcinoma. The antitumor effect of TAC-101 alone or combined with cisplatin was tested using human ovarian carcinoma.

Methods. Induction of genes related to apoptosis by TAC-101 or cisplatin was assessed by DNA microarray analysis. TAC-101 (8 mg/kg/day orally for 21 days), cisplatin (7 mg/kg intravenously on day 1), or a combination of both drugs at the same dosages was administered to nude mice implanted subcutaneously with RMG-I or RMG-II clear cell adenocarcinoma cells. The antitumor effect was evaluated by calculating the treated/control tumor volume ratio at 21 days after implantation. The histoculture drug response assay was also performed using fresh surgical specimens of human ovarian cancer to determine the 50% inhibitory concentration (IC_{50}).

Results. Different apoptosis-related genes were induced by TAC-101 and cisplatin. Compared with control mice, the volume of both RMG-I and RMG-II tumors was significantly reduced ($p<0.05$) by either drug. The IC_{50} values of cisplatin and TAC-101 showed a significant correlation ($p<0.01$).

Conclusion. These *in vitro* findings suggest that a combination of TAC-101 and cisplatin may be a potential new treatment for ovarian clear cell adenocarcinoma.

Keywords: Ovarian carcinoma; Clear cell adenocarcinoma; TAC-101; Cisplatin; Histoculture drug response assay

Introduction

Clear cell adenocarcinoma accounts for more than 10% of ovarian cancer [1] and its incidence has recently been increasing in Japan [2]. Up to 60% of patients with this tumor have stage I disease according to the International Federation of Gynecology and Obstetrics (FIGO) classification [3]. However, patients with clear cell adenocarcinoma have a poor prognosis even when it is diagnosed at an early stage and treated by complete resection [2,4]. Since clear cell adenocarcinoma seems to show resistance to platinum-based chemotherapy, unlike the other types of ovarian carcinoma [5], more effective chemotherapy is needed for this tumor.

Retinoids have great potential in the fields of cancer therapy and chemoprevention [6,7]. While some tumor cells are sensitive to the growth inhibitory effects of natural retinoids, such as all-*trans*-retinoic acid (ATRA), many ovarian tumor cells are not [8]. We previously found that a new synthetic retinoid, 4-[3,5-bis (trimethylsilyl) benzamido] benzoic acid (TAC-101) was more effective at inducing apoptosis of clear cell adenocarcinoma cell lines than it was for other histological types of ovarian carcinoma [9]. TAC-

* Corresponding author. Fax: +81 3 3226 1667.
E-mail address: aoki@sc.itc.keio.ac.jp (D. Aoki).

0090-8258/$ - see front matter © 2007 Elsevier Inc. All rights reserved.
doi:10.1016/j.ygyno.2007.10.019

101 also inhibits the growth of xenografts of a human ovarian clear cell adenocarcinoma cells (RMG-II), similar to paclitaxel, and has a stronger effect than *cis*-diammine dichloroplatinum (cisplatin) [9]. In the present study, we assessed the antitumor effect of cisplatin combined with TAC-101, as well as that of each drug alone. We analyzed the induction of genes related to apoptosis by each drug because TAC-101 might have different antitumor activity from cisplatin due to differences in their influence on gene expression. We also used an *in vivo* assay to determine the effect of TAC-101 or cisplatin on clear cell adenocarcinoma in mice, as well as the response to both agents combined. Finally, the histoculture drug response assay (HDRA) was performed to compare the activity of TAC-101 and cisplatin against human ovarian cancer specimens.

The results of these investigations were used to assess the potential clinical value of combined therapy with TAC-101 and cisplatin for ovarian clear cell adenocarcinoma, which has a poor prognosis due to resistance to standard platinum-based chemotherapy [5].

Materials and methods

Chemicals

TAC-101 was provided by Taiho Pharmaceutical Co., Ltd. (Saitama, Japan), cisplatin was purchased from Nippon Kayaku Co., Ltd. (Tokyo, Japan), and ATRA was purchased from Sigma Chemical Co. (MO, USA). For *in vitro* experiments, TAC-101 and ATRA were dissolved in dimethyl sulfoxide at concentrations of 20 mM and 10 mM to make stock solutions, which were stored at −20 °C until use. For *in vivo* experiments, TAC-101 was suspended in 0.5% hydroxyl propylmethylcellulose (Shin-Etsu Chemical Co., Ltd., Tokyo, Japan).

Cell culture

Two human ovarian clear cell adenocarcinoma cell lines (RMG-I and RMG-II), which we previously established [10,11], were cultured in a Ham's F 12 medium (Gibco Laboratories, NY, USA) supplemented with 10% fetal calf serum (FCS) (Mitsubishi Chemical Co., Tokyo, Japan) and 80 μg/ml of kanamycin sulfate (Meiji Seika Kaisha Ltd., Tokyo, Japan) at 37 °C under an atmosphere of 5% CO_2.

Microarray analysis

RMG-I and RMG-II cells (1×10^6 cells) were seeded into 10-cm flasks (BD Bioscience, MA, USA) and incubated for 3–5 days, after which the medium was replaced with fresh medium containing cisplatin (7.5 μg/ml),or TAC-101 (25 μM), and 2% FCS (control). Cultured cells were harvested after 24 h later.

Total RNA was extracted from these flasks using an RNeasy column (Quagen, CA, USA). Then microarray gene analysis was performed using a human apoptosis GEArray Q series kit (Super Array Co., MD, USA) consisting of 96 apoptosis-related genes and 4 housekeeping genes printed on a membrane. Total RNA (0.5 μg) was used as a template for the synthesis of biotin/dUTP-labeled cDNA probes according to the manufacturer's protocol. Membranes were hybridized with the labeled probes, washed, treated with 1.0 ml of CDP-Star chemiluminescence solution, and exposed to X-ray film (Eastman Kodak Company, NY, USA). Image analysis software (Scananalyze and GEArray Analyzer, Super Array Co., MD, USA) was employed to assess gene expression, and the increase in expression of apoptosis-related genes relative to the control (culture with FCS alone) was analyzed by Student's *t*-test. Expression of GAPDH was also assessed as a house-keeping gene. Anti-sense cDNAs for each gene were placed on the same GEArray chip from two to four times and average values were calculated. The expression of each gene was normalized by subtracting the background value and dividing by the level of GAPDH expression. Expression of each gene was measured twice by the same method and data were analyzed by the paired *t*-test with regard to the differences of population mean values between two related groups. For genes that showed significant differences of expression, their ratio relative to control expression was calculated. A ratio ≥ 1.5 was defined as up-regulation and a ratio $\leq 2/3$ was defined as down-regulation.

Activity against RMG-I and RMG-II tumors in nude mice

RMG-I or RMG-II cells were implanted subcutaneously into the backs of nude mice, and the tumors that developed were measured after 3 weeks. Mice that had tumors with an estimated volume ([largest diameter (mm) × smallest diameter (mm)]^2/2) of approximately 100 mm^3 were selected and assigned to groups of 8 animals each by stratified random allocation based on the individual tumor volumes, so that each group had a almost equal mean tumor volume on day 1. Changes in the body weight of the mice were measured to determine the nontoxic dose of each drug, and inhibition of tumor growth was examined at that dose.

TAC-101 (8 mg/kg/day) was administered daily for 21 days by oral gavage using a 1-ml tuberculin syringe (SS-01T, Terumo Co., Tokyo, Japan) and needle, while cisplatin was injected into the tail vein at a dose of 7 mg/kg on day 1. Combination therapy was given with TAC-101 and cisplatin at these doses. The dose of TAC-101 was set on the basis of its antiproliferative activity and effect on body weight in a previous dose-finding study [12], while the dose of cisplatin was equivalent to that used clinically [13]. An untreated control group was also included. Body weight was measured twice a week in order to monitor toxicity. Animals were handled in accordance with the protocol established by the Animal Care Committee of Taiho Pharmaceutical Co., Ltd. (Tokyo, Japan).

The tumor volume (TV) was measured daily over time in each animal and the ratio of the volume on day 21 to that at the start of treatment was calculated. Welch's *t*-test (two-tailed) was performed to compare TV values and the effect of combined treatment was determined by the intersection union test [14].

Histoculture drug response assay (HDRA)

Among patients who underwent surgery for ovarian cancer at Keio University Hospital, the HDRA was performed in those who consented to enrollment in the present study. The study protocol was approved by our IRB (institutional review board), and informed consent was obtained from all participating patients. We performed the HDRA (TAC-101 32 cases, ATRA 27 cases, cisplatin 33 cases) according to a modification of the method of Ohic et al. [15]. Briefly, collagen gel sponge (Gel Foam, Pharmacia & Upjohn Co., Tokyo, Japan) was cut into cubes of about 1 mm^3, and a cube was placed into each well of a 24-well plate (Sumilon, Sumitomo Bakelite Co., Ltd., Tokyo, Japan). The culture medium (1 ml/well) was F-12 medium (Gibco Laboratories, NY, USA) containing 20% fetal bovine serum (Mitsubishi Chemical, Co., Tokyo, Japan) and 80 μg/ml of kanamycin (Meiji Seika Kaisha, Ltd., Tokyo, Japan). The concentration of cisplatin (Nippon Kayaku, Co. Ltd., Tokyo, Japan) in the culture medium was set at 6.25, 12.5, 25, 50, or 100 μg/ml, and each concentration was tested in 4 wells. The same concentrations of TAC-101 (Taiho Pharmaceutical Co., Ltd., Tokyo, Japan) and ATRA (Sigma Chemical Co., MO, USA) were also tested in 4 wells each. During surgery, tumor specimens were harvested aseptically and cut into cubes of approximately 1 mm^3 with scissors. Then a tumor tissue cube was placed onto the collagen sponge in each well of the 24-well plate. After incubation at 37 °C under an atmosphere of 5% CO_2 for 7 days, viable cells were detected by the methylthiazoletetrazolium (MTT) assay. In brief, MTT (Sigma Chemical Co., MO, USA) was dissolved in phosphate-buffered saline (5 mg/ml) containing 100 mM succinic acid (Wako Pure Chemical Industries, Ltd., Tokyo, Japan). Then 100 μl of MTT solution was added to each well, and incubation was done for 4 h at 37 °C under an atmosphere of 5% CO_2. The stained tumor tissue cubes were subsequently transferred into new 24-well plates, after which 1 ml of dimethyl sulfoxide (Wako Pure Chemical Industries, Ltd., Tokyo, Japan) was added to extract the MTT-formazan product. Next, 100 μl of the extract from each well was transferred into the wells of a 96-well microplate (Sumilon, Sumitomo Bakelite Co., Ltd., Tokyo, Japan), and the absorbance was measured at 540 nm using a microplate reader (Model 450, Bio-Rad Laboratories, CA, USA). After

Table 1
Up-regulated genes

	TAC-101			Cisplatin		
	Gene name	Ratio	*p*-value	Gene name	Ratio	*p*-value
RMG-I	RIP	14.51	<0.05	Bcl-10	1.91	0.06
	Cardiac/RIP2	7.17	0.08	IAP-2	1.67	<0.05
	CHK2	6.98	0.06			
	Caspase 5	5.05	<0.05			
	CIDE-A	4.03	<0.05			
	LTBR	2.11	<0.05			
	LTB	2.09	<0.05			
	p63	2.00	0.08			
	NAIP/BIRCI	1.94	0.10			
	TNFB	1.72	0.06			
	PYCARD	1.52	0.08			
RMG-II	Caspase 5	2.17	<0.05	Bcl-2	2.82	0.08
				Caspase 5	1.65	<0.05

RIP: receptor-interacting protein.
Cardiac/RIP2: cardiac/receptor-interacting protein-2.
CHK2: checkpoint kinase 2.
CIDE-a: cell death-inducing DFFA-like effector-A.
LTBR: lymphotoxin-beta receptor.
LTB: lymphotoxin-beta.
TNFB: tumor necrosis factor-beta.
PYCARD: PYD and CARD domain-containing protein.
IAP-2: inhibitor of apoptosis protein-2.

extraction of the formazan product, the wet weight of the tumor tissue was also measured and the absorbance per gram of tissue was calculated. The percent inhibition of tumor growth by each drug was calculated by comparison with the growth in untreated control wells using the following formula: Percent inhibition of tumor growth (%)=[1−(absorbance per gram of tumor tissue in treated wells/absorbance per gram of tumor tissue in control wells)]×100.

To determine whether TAC-101, cisplatin, and ATRA showed activity against a tumor, the 50% inhibitory concentration (IC_{50}) of each drug was calculated. Spearman's correlation coefficient analysis was used to examine correlations between the IC_{50} values for TAC-101 or ATRA and the values for cisplatin.

Results

Effect of TAC-101 and cisplatin on clear cell adenocarcinoma cell lines

As shown in Tables 1 and 2, microarray analysis of RMG-I and II cells revealed differences in the expression of apoptosis-related genes between TAC-101 and cisplatin treatment. RMG-I and -II cells were both tested twice under the same conditions to select genes that showed significant changes of expression compared with control culture (no agents).

Table 2
Down-regulated genes

	TAC-101			Cisplatin		
	Gene name	ratio	*p*-value	Gene name	ratio	*p*-value
RMG-II	TRAIL-R4	0.59	0.07	PYCARD	0.66	<0.05
	IAP-2	0.58	<0.05	Caspase 14	0.55	0.07
	Hus1	0.35	0.07	Caspase 9	0.16	<0.05
	CHK1	0.31	0.08			
	TNF-alpha	0.06	<0.05			
	TRAF6	0.04	0.09			

TRAIL-R4: tumor necrosis factor receptor superfamily.
Hus1: hydroxyurea-sensitive (check point homolog).
CHK1: checkpoint.
TNF-alpha: tumor necrosis factor-alpha.
TRAF6: TNF receptor-associated factor 6.

In RMG-I cells, the apoptosis-related molecules up-regulated by addition of TAC-101 were receptor-interacting protein (RIP), caspase 5, cell death-inducing DFFA-like effector A (CIDE-A), lymphotoxin-beta receptor (LTBR), and lymphotoxin receptor (LTB). In contrast, the only apoptosis-related molecule up-regulated by addition of cisplatin was inhibitor of apoptosis protein-2 (IAP-2). In RMG-I cells, no apoptosis-related molecules were significantly down-regulated by either of the two drugs.

In RMG-II cells, the apoptosis-related molecule up-regulated by addition of either TAC-101 or cisplatin was CAS5. In RMG-II cells, the apoptosis-related molecules down-regulated by addition of TAC-101 were IAP-2 and TNF-alpha, while the molecules down-regulated by addition of cisplatin were PYD and CARD domain-containing protein (PYCARD) as well as caspase 9.

Effect of TAC-101 and cisplatin on xenografts in mice

On day 21, that TAC-101 suppressed the tumor growth the most, after implantation of RMG-I cells, the treated/control ratio of the relative tumor volume (RTV=mean TV in the treated group/mean TV in the control group)×100) was 73%, 73%, and 48% in the TAC-101 monotherapy group, cisplatin monotherapy group, and combined therapy group, respectively (Table 3). Compared with the control group and combination therapy, the RTV was significantly smaller in the combined therapy group ($p<0.01$, Welch's *t*-test). When the effect of each drug treated group was assessed (the intersection union test), RTV was found to be significantly decreased by TAC-101 monotherapy ($p<0.05$) and also by cisplatin monotherapy ($p<0.05$) compared with combination therapy. For RMG-II cells, the treated/control RTV ratio on day 21 was 68%, 80%, and 60% in the

Table 3
Activity against RMG-I tumors in nude mice ($n=8$)

	TV on day21 (Mean±2SD)(mm^3)	RTV (%)
C	6.26±2.05	100
T	4.55±1.60	73
P	4.55±1.76	73
T/P	2.98±0.88	48

*$p<0.05$, **$p<0.01$, by Welch's test.

Table 4
Activity against RMG-II tumors in nude mice ($n=8$)

	TV on day21 (Mean±2SD)(mm^3)	RTV (%)
C	3.54±1.21	100
T	2.41±0.47	68
P	2.85±0.59	80
T/P	2.13±0.57	60

*$p<0.05$, **$p<0.01$, by Welch's test.

Table 5
Results of Spearman's rank correlation coefficient analysis of HDRA data

	TAC-101 vs. cisplatin ($n=31$)	TAC-101 vs. ATRA ($n=24$)	Cisplatin vs. ATRA ($n=25$)
Results of the test	Positive correlation	No correlation	No correlation
Sum of square of rank difference	2626	2202	1732
Correlation coefficient rs	0.47	0.04	0.33
Z value	2.58	0.20	1.64
p-value (two-sided probability)	$p<0.01$	$p=0.84$	$p=0.10$

TAC-101 monotherapy group, the cisplatin monotherapy group, and the combination therapy group, respectively (Table 4). Compared with the control group, RTV was significantly decreased in both the TAC-101 monotherapy group and the combined therapy group (Welch's t-test: $p<0.05$ and $p<0.01$, respectively). When compared between groups which the drug used (the intersection union test) to assess the effect of those, only the cisplatin monotherapy group showed a significant decrease of RTV ($p<0.05$) compared with the combination therapy group. Body weight was monitored by measuring the average weight and the average change of weight in each group of mice. Weight loss of 15% or more indicating severe drug toxicity which is out of evaluation of antitumor activity was not detected in this study.

Effect of TAC-101 and cisplatin on surgical specimens of ovarian cancer

The IC_{50} values of TAC-101, cisplatin, and ATRA (control) were determined, and correlations were investigated by Spearman's correlation coefficient analysis.

As a result, the IC_{50} of TAC-101 showed a significant correlation with that of cisplatin ($rs=0.47$, $p<0.01$), but the IC_{50} of ATRA was not correlated with that of cisplatin ($rs=0.33$, $p=0.10$) (Table 5).

Discussion

Clear cell adenocarcinoma accounts for slightly more than 10% of all epithelial ovarian carcinoma according to FIGO [1]. In recent years, however, an increase of this type of tumor has occurred in Japan and it now accounts for about 20% of ovarian carcinoma [2]. The combination of paclitaxel and carboplatin which is a standard chemotherapy so far only achieves a low response rate of 18% and most tumors show resistance to currently available chemotherapy, resulting in a poor prognosis, thus there is an urgent need for more effective treatment [2].

We previously found that TAC-101 induces the apoptosis of various ovarian cancer cells [9], particularly RMG-I and RMG-II cells derived from clear cell adenocarcinoma. TAC-101 has also demonstrated antitumor effect comparable to that of paclitaxel and cisplatin against clear cell adenocarcinoma xenografts in nude mice [9]. Furthermore, TAC-101 shows antitumor activity against colon cancer cells [16], but its mechanism of action has not yet been elucidated for either type of cancer. Because TAC-101 induces apoptosis, we focused on apoptosis-related genes in the present study to investigate the potential mechanism of its antitumor effect. When DNA microarray analysis was performed, up-regulation of caspase 5 was found as an effect of TAC-101 and cisplatin, but was not seen with ATRA. These results are in agreement with our previous *in vitro* findings that cisplatin and TAC induce apoptosis, but ATRA does not [9], suggesting that the anticancer effect of TAC-101 and cisplatin is based on induction of apoptosis.

Although Sako et al. [17] found that TAC-101 caused up-regulation of FAS in colon cancer cells, there was no relationship between this change and induction of apoptosis by TAC-101 in ovarian clear cell adenocarcinoma based on our results obtained using RMG-I and RMG-II cells.

Microarray analysis of RMG-I and RMG-II cells revealed differences in the expression of apoptosis-related genes between TAC-101 and cisplatin. TAC-101 induced the expression of pro-apoptotic molecules such as RIP, caspase 5, CIDE-A, and TNF-alpha, while it inhibited the expression of IAP-2, an anti-apoptotic molecule, suggesting possible induction of apoptosis in ovarian clear cell adenocarcinoma cells.

In contrast, cisplatin up-regulated some anti-apoptotic factors, such as IAP and Bcl family genes, and it down-regulated pro-apoptotic factors like caspase 9. Such changes of gene expression may be related to the resistance of clear cell adenocarcinoma to cisplatin and platinum-based chemotherapy, unlike the other types of epithelial ovarian carcinoma [5]. The possibility of enhanced efficacy by concomitant administration of TAC-101 with cisplatin could also be suggested because these two drugs have different mechanisms for the induction of apoptosis. To make matters clearer and pursue the issue, further discussion is needed on the apoptotic genes and their significance on the findings as related to apoptosis; particularly, how the findings of TAC-101 suggest induction of apoptosis.

The present study also demonstrated that TAC-101 was able to inhibit the growth of clear cell adenocarcinoma tumors in mice, with the RTV being reduced to 73% and 68% of the control value for RMG-I and RMG-II tumors, respectively, while the respective values were 73% and 80% in the case of cisplatin monotherapy. Thus, TAC-101 demonstrated a similar effect to cisplatin, which is recognized as a key chemotherapy agent for ovarian carcinoma. When the combined effect of these drugs was evaluated, there was a significant decrease of tumor volume, suggesting that the combination of cisplatin and TAC-101 may be a potential new treatment for clear cell adenocarcinoma.

Although a clinical study of TAC-101 is currently underway [18], its activity against human ovarian carcinoma is still unknown. Therefore, we performed the HDRA to investigate the antitumor activity of TAC-101 against human ovarian carcinoma specimens. We previously used the HDRA to assess the response of cisplatin for ovarian carcinoma, and we found a true positive rate, true negative rate, and accuracy of 88%, 86%, and 87%, respectively [19]. We have also found that the clinical efficacy of cisplatin therapy for ovarian carcinoma can be predicted by the HDRA [19]. When patients were classified into high-sensitivity and low-sensitivity groups based on the cut-off IC_{50} value for cisplatin and the 5-year overall survival rate was

compared by the Kaplan–Meier method, it was significantly higher in the high-sensitivity group than in the low-sensitivity group [19]. Because it is not currently possible to obtain such clinical data of ovarian cancer patients for TAC-101, its effect on ovarian specimen was indirectly evaluated by comparing IC_{50} values with those for cisplatin. We found that the IC_{50} values for TAC-101 and cisplatin determined in the HDRA showed a significant positive correlation ($p<0.01$). Accordingly, the two drugs may demonstrate a synergistic effect on tumors showing a high sensitivity to cisplatin in the HDRA, because of the difference in their apoptosis-inducing effect (microarray analysis) and the stronger activity demonstrated against implanted RMG-I and RMG-II tumors by a combination of these two drugs. Further investigation is still necessary, but clinical activity of TAC-101 against ovarian carcinoma is possible based on the results of the HDRA.

In conclusion, our findings suggest that the combination of TAC-101, an orally active synthetic retinoid, and cisplatin may be a potential new treatment for clear cell adenocarcinoma.

Acknowledgment

The authors thank Ms. Keiko Abe for preparing the manuscript.

References

[1] Alexander WK, Charles VB, William RH. Ovarian clear cell adenocarcinoma. Gynecol Oncol 1989;32:342–9.
[2] Enomoto T, Kuragaki C, Yamasaki M, et al. Is clear cell carcinoma and mucinous carcinoma of the ovary sensitive to combination chemotherapy with paclitaxel and carboplatin? Proc Am Soc Clin Oncol 2003;22:447.
[3] Tsunehisa K, Shinji O, Yoshiaki K, et al. Histological classification of ovarian cancer. Med Electron Microsc 2003;36:9–17.
[4] Monga M, Carmichael JA, Shelly WE. Surgery without adjuvant chemotherapy for early epithelial ovarian carcinoma after comprehensive surgical staging. Gynecol Oncol 1991;43:195–7.
[5] Hakes TB. Prognostic factors in ovarian cancer. In: Markman M, Hoskins WJ, editors. Cancer of the ovary. New York: Raven Press; 1993. p. 115–26.
[6] Mjuindi J, Frankel S, Huselton C, et al. Clinical pharmacology of oral all-trans retinoic acid in patients with acute promyelocytic leukemia. Cancer 1992;52:2138–42.
[7] Silverman A, Ellis C, Voorhees J. Hypervitaminosis A syndrome: a paradigm of retinoid side effects. J Am Acad Dermatol 1987;16:1027–39.
[8] Holmes WF, Soprano DR, Soprano KJ. Synthetic retinoids as inducers of apoptosis in ovarian carcinoma cell lines. J Cell Physiol 2004;199:317–29.
[9] Suzuki N, Aoki D, Ohie S, et al. A novel retinoid, 4-[3,5-bis (trimethylsilyl) benzamido] benzoic acid (TAC-101), induces apoptosis of human ovarian carcinoma cells and shows potential as a new antitumor agent for clear cell adenocarcinoma. Gynecol Oncol 2004;94:643–9.
[10] Nozawa S, Tsukazaki K, Sakayori M, Jeng CH, Iizuka R. Establishment of a human ovarian clear cell carcinoma cell line (RMG-I) and its single cloning. Hum Cell 1988;1:426–35.
[11] Nozawa S, Yajima M, Sasaki H, et al. A new CA-125-like antigen (CA602) recognized by two monoclonal antibodies against a newly established ovarian clear cell carcinoma cell line (RMG-II). Jpn J Cancer Res 1991;82:854–61.
[12] Murakami K, Werzba K, Sano M, et al. TAC-101, a benzoic acid derivative, inhibits liver metastasis of human gastrointestinal cancer and prolongs the lifespan. Clin Exp Metastasis 1998;16:323–31.
[13] Nomura T, Sakurai Y, Inaba M. The nude mouse and anticancer drug evaluation. Tokyo: Chemotherapy Publishers Inc.; 1996.
[14] Berger Roger L, Hsu Jason C. Bioequivalence trials, intersection-union tests and equivalence confidence sets. Stat Sci 1996;11(4):283–319.
[15] Ohie S, Udagawa Y, Kozu A, et al. CDDP sensitivity of ovarian cancer in the histoculture drug response assay correlates to clinical response to combination chemotherapy with CDDP, doxorubicin and cyclophosphamide. Anticancer Res 2000;20:2049–54.
[16] Sakukawa R, Murakami K, Ikeda T, Yamada Y, Saiki I. Effect of 4-[3,5-bis (trimethylsilyl) benzamido] benzoic acid (TAC-101) on the liver metastasis of colon 26-L5 carcinoma cells. Oncol Res 1998;10:287–93.
[17] Sako T, Nakayama Y, Minagawa N, et al. 4-[3,5-bis (trimethylsilyl) benzamido] benzoic acid (TAC-101) induces apoptosis in colon cancer partially through the induction of Fas expression. In Vivo 2005;19: 125–32.
[18] Rizvi NA, Marshall JL, Ness E, et al. Initial clinical trial of oral TAC-101, a novel retinoic acid receptor-alpha selective retinoid, in patients with advanced cancer. J Clin Oncol 2002;20:3522–32.
[19] Nakada S, Aoki D, Ohie S, et al. Chemosensitivity testing of ovarian cancer using the histoculture drug response assay: sensitivity to CDDP and clinical response. Int J Gynecol Cancer 2005;15:445–52.

Establishment of an ovarian metastasis model and possible involvement of E-cadherin down-regulation in the metastasis

Yoshiko Kuwabara,[1,2] Taketo Yamada,[1] Ken Yamazaki,[1] Wen-Lin Du,[1] Kouji Banno,[2] Daisuke Aoki[2] and Michiie Sakamoto[1,3]

Departments of [1]Pathology and [2]Obstetrics and Gynecology, School of Medicine, Keio University, 35 Shinanomachi, Shinjuku-ku, Tokyo 160-8582, Japan

(Received February 28, 2008/Revised June 14, 2008/Accepted June 24, 2008/Online publication October 3, 2008)

Clinical observations of cases of ovarian metastasis suggest that there may be a unique mechanism underlying ovarian-specific metastasis. This study was undertaken to establish an *in vivo* model of metastasis to the ovary, and to investigate the mechanism of ovarian-specific metastasis. We examined the capacity for ovarian metastasis in eight different human carcinoma cell lines by implantation in female NOD/SCID mice transvenously and intraperitoneally. By transvenous inoculation, only RERF-LC-AI, a poorly differentiated carcinoma cell line, frequently demonstrated ovarian metastasis. By intraperitoneal inoculation, four of the eight cell lines (HGC27, MKN-45, KATO-III, and RERF-LC-AI) metastasized to the ovary. We compared E-cadherin expression among ovarian metastatic cell lines and others. All of these four ovarian metastatic cell lines and HSKTC, a Krukenberg tumor cell line, showed E-cadherin down-regulation and others did not. E-cadherin was then forcibly expressed in RERF-LC-AI, and inhibited ovarian metastasis completely. The capacity for metastasizing to the other organs was not affected by E-cadherin expression. We also performed histological investigation of clinical ovarian-metastatic tumor cases. About half of all ovarian-metastatic tumor cases showed loss or reduction of E-cadherin expression. These data suggest that E-cadherin down-regulation may be involved in ovarian-specific metastasis. (*Cancer Sci* 2008; 99: 1933–1939)

Metastasis is the major cause of death from cancer, despite significant progress in the diagnosis and clinical management of the diseases. It is urgent and essential to elucidate the mechanisms of cancer metastasis in order to improve the prognosis of cancer patients. Generally, metastasis consists of multiple events initiating invasion to the basement membrane and connective tissue, followed by migration into an adjacent blood or lymphatic vessels and the reaching of distant organs. The last step in metastasis is the arrest of circulating cancer cells and formation of tumor foci at the target organ.[1–4] Two mechanisms have been proposed underlying the multiple steps of metastasis.[5,6] One theory, that floating cancer cells in the blood or lymphatic stream are trapped in capillary vessels by mechanical constraints and grow to form secondary foci, simply correlates with the blood or lymphatic flow pattern. Metastasis of colon cancer to the liver may follow this anatomical theory, for instance; however, the other is a more complicated hypothesis based on molecular interactions between cancer cells (seeds) and the microenvironment of the target organ (soil). This 'seed and soil' theory can explain organ-specific metastasis such as the bone metastasis of prostate cancer,[7] brain metastasis of breast cancer,[8] and so on.

The incidence of metastatic ovarian tumors has been reported to comprise 7–10% of all ovarian cancer.[9,10] The common sources of ovarian metastatic tumors are the stomach, colon and rectum, appendix, breast, uterus, lung, and skin (melanoma).[11–14] Interestingly, bilateral lesions are found in 50–70% of patients,[10–12] and there are several reports of cases of intramucosal gastric cancers with ovarian metastasis.[15,16] These clinical data, which indicate the propensity of some tumor subsets for metastasis to the ovary, suggest the existence of unknown mechanisms underlying ovarian-specific metastasis.

Among metastatic tumors in the ovary, there is an interesting and controversial subset of tumors named Krukenberg tumors. The term 'Krukenberg tumor' has sometimes been loosely applied to any adenocarcinoma metastasizing to the ovary; however, most investigators used the classical criteria for the diagnosis of Krukenberg tumor as follows: (1) cancer in the ovary; (2) intracellular mucin production by neoplastic signet-ring cells; and (3) diffuse sarcomatoid proliferation of ovarian stroma.[17,18] The mechanisms that develop these morphologic alterations are not clear, but the significant stromal proliferation suggests that some tumor–stroma interactions may be involved in ovarian-specific metastasis.

To elucidate the mechanisms underlying ovarian-specific metastasis, an *in vivo* model of ovarian metastasis is definitely needed. To date, however, such a model has never been established. In our experiments, eight different human carcinoma cell lines were implanted in immune-deficient mice by transvenously and intraperitoneally. We examined the capacity for ovarian metastasis of these cell lines, and succeeded in establishing an *in vivo* ovarian-metastasis model with stromal reaction in the ovarian tumor. We further investigated whether E-cadherin down-regulation might be involved in ovarian-specific metastasis, because all cell lines revealing some capacity for metastasis to the ovary showed loss or reduction of E-cadherin expression.

Materials and Methods

Cell cultures. We used eight human carcinoma cell lines, as shown in Table 1. The characteristics and origins of MKN-28, MKN-45, MKN-74, TMK-1, and KATO-III are described elsewhere.[19,20] HGC27, HSKTC,[21] and RERF-LC-AI were purchased from RIKEN BioResource Center, Japan. HGC27 and RERF-LC-AI were maintained in MEM (Gibco/Invitrogen, Carlsbad, CA, USA) with 10% fetal bovine serum (FBS; PAA Laboratories, Ontario, Canada). HSKTC were maintained in F-12 HAM (Sigma-Aldrich, St. Louis, MO, USA) with 15% FBS and 2-mM L-glutamine. The other cell lines were maintained in RPMI-1640 (Sigma-Aldrich) with 10% FBS. All media were also supplemented with 100-μg/mL ampicillin and 100-μg/mL streptomycin. All cells were incubated at 37°C under 5% CO_2 and harvested from subconfluent cultures.

[3]To whom correspondence should be addressed.
E-mail: msakamot@sc.itc.keio.ac.jp

doi: 10.1111/j.1349-7006.2008.00946.x

Table 1. Human carcinoma cell lines inoculated into mice

Cell line	Origin
HGC27	Poorly differentiated gastric carcinoma
TMK-1	Poorly differentiated gastric carcinoma
MKN-45	Poorly differentiated gastric carcinoma
MKN-28	Moderately differentiated gastric carcinoma
MKN-74	Moderately differentiated gastric carcinoma
KATO-III	Gastric signet ring cell carcinoma
HSKTC	Krukenberg tumor
RERF-LC-AI	Poorly differentiated lung carcinoma

Animals. NOD/SCID (NOD/LtSz-scid) mice were maintained in a specific pathogen-free environment. Six- to 8-week-old mice were used in this experiment. Studies were conducted in accordance with the National Institutes of Health Guide for the Care and Use of Laboratory Animals.

Metastatic screening assays. Cells were suspended in the corresponding medium and inoculated into mice by injection into the tail vein (1×10^6 cells in 100 μL per mouse) and peritoneal cavity (1×10^7 cells in 100 μL per mouse). Mice were sacrificed when they became moribund and were evaluated for the organ distribution of established tumors. All experiments were performed under appropriate anesthesia. The resected tissues were fixed in 10% formalin, cut into 2- to 3-mm-thick slices, and embedded in paraffin for subsequent histological examination.

Immunoblotting. Cells were lysed in a buffer consisting of 25 mmol/L Tris-HCl (pH 8.0), 5 mmol/L ethylenediaminetetraacetic acid (EDTA), 125 mmol/L NaCl, 0.5% Triton X-100, 0.5% NP-40 (Sigma-Aldrich), and protease inhibitor mixture (Roche Diagnostics). After centrifugation at 20400g for 15 min, the supernatant was obtained. All 30-μg cell lysates were subjected to sodium dodecyl sulfate–polyacrylamide gel electrophoresis and then separated proteins were transferred to Hybond-P (Amersham Biosciences, Buckinghamshire, UK). After blocking, an anti-E-cadherin mouse monoclonal antibody (dilution 1:2500; Becton Dickinson, NJ, USA) or anti-β-actin mouse monoclonal antibody (dilution 1:1000; Sigma-Aldrich) was incubated for 1 h at room temperature. The membrane was incubated with a horseradish peroxidase–conjugated secondary antibody (Dako, Glostrup, Denmark) and visualized using an enhanced chemiluminescence kit (Amersham Biosciences).

Transfection. A PEF1/Myc-His vector plasmid containing the murine E-cadherin gene or an empty vector plasmid (kindly provided by Dr Shibata at the National Cancer Center Research Institute, Tokyo, Japan) was transfected into RERF-LC-AI using the Lipofectamine LTX Reagent (Invitrogen) according to the manufacturer's protocol. A neomycin resistance gene on the vectors was used to create geneticin-resistant stable clones.

Immunofluorescence. RERF-LC-AI and its transfectant clones were grown on collagen type I-coated culture slides (Becton Dickinson) and fixed in 4% formalin for 10 min. They were permealized with 0.1% Triton-X-100, blocked in 5% normal rabbit serum, and incubated with an anti-E-cadherin mouse monoclonal antibody overnight at 4°C, followed by an fluorescein-isothiocyanate–labeled secondary antibody (Dako) for 30 min at room temperature. The primary antibody was used at 1:100 and the secondary antibody at 1:50 dilution in 5% normal rabbit serum. Texas Red-X phalloidin (Molecule Probes, Eugene, OR, USA) and Hoechst (Molecule Probes) were used to visualize filamentous actin and the nucleus, respectively. Slides were examined using a Zeiss confocal laser scanning microscope (Axiovert 200 M LSM510-Software; Carl Zeiss, Göttingen, Germany).

Patients and tissue samples. To investigate clinical ovarian metastatic tumor cases, 25 operated cases and five autopsies were analyzed. In all cases, macroscopic enlargement of the ovary was observed. Sections were prepared from formalin-fixed, paraffin-embedded tissues of samples resected surgically between 1989 and 2005. This study was conducted under the approval of the Ethics Committee of Keio University, School of Medicine.

Immunohistochemistry. Each section was deparaffinized, rehydrated, and incubated with fresh 0.3% hydrogen peroxide in methanol for 30 min at room temperature. For antigen retrieval, sections were boiled in pH 6 (E-cadherin staining of mouse samples) or pH 7 (smooth muscle actin [SMA] staining and human-specific cytokeratin; CAM 5.2) citrate buffer for 10 min, or autoclaved in pH 7 citrate buffer (E-cadherin staining of human samples), or incubated in 0.1% tripsin at 37°C for 20 min (pankeratin staining). The sections were then incubated with primary antibodies for 1 h at room temperature. The primary antibodies and dilutions were as follows: anti-E-cadherin monoclonal antibody (1:5000; BD Transduction Laboratory) for mouse samples, anti-E-cadherin monoclonal antibody (1:500; HECD1[22]) for human samples, anti-AE1/AE3 monoclonal antibody (1:200; Dako), anti-SMA monoclonal antibody (1:200; Dako), and anti-CAM 5.2 monoclonal antibody (1:20; BD Transduction Laboratory). The sections were washed three times in phosphate-buffered saline, and incubated with the secondary antibody, Immpress Reagent (Vector Laboratories), for 30 min at room temperature.

Statistical analysis. The ages of the patients with clinical ovarian metastatic tumor were compared using the Mann–Whitney *U*-test. Other correlations were analyzed by the χ^2-test. All calculations were performed with ystat2000 (Igaku Tosho Shuppan, Tokyo, Japan).

Results

Examination of the capacity for ovarian metastasis in the eight cell lines and establishment of an ovarian-metastasis model. Using transvenous inoculation to NOD/SCID mice, the tumorigenicity of the eight human cancer cell lines was extremely low in our examination. Almost all cell lines did not show any tumorigenicity, including in the lung or liver. Only RERF-LC-AI, however, formed tumors in several organs (Table 2). RERF-LC-AI metastasized to the lung at 100%, which was considered to be a natural result because this cell line was originally derived from a lung cancer, and also because the lung should generally be the first organ that cells reach after injection into the tail vein. RERF-LC-AI most frequently metastasized to the ovary (67%) after the lung, and bilateral lesions were observed in one-third of ovarian metastatic cases (Table 2, Fig. 1a). Therefore, it was considered that RERF-LC-AI had a high propensity for ovarian metastasis, and that the experimental system of transvenous inoculation of this cell line to NOD/SCID mice could be used

Table 2. Organ distribution of experimental metastasis after transvenous inoculation of RERF-LC-AI

Organ							Days after inoculation
Ovary (unilateral/bilateral)	Peritoneal dissemination	Ascites	Pancreas	Liver	Lung	Bone/bone marrow	
3/5 (60%) (2/1)	1/5 (20%)	0/5 (0%)	1/5 (20%)	0/5 (0%)	5/5 (100%)	1/3 (33%)	53–94

doi: 10.1111/j.1349-7006.2008.00946.x

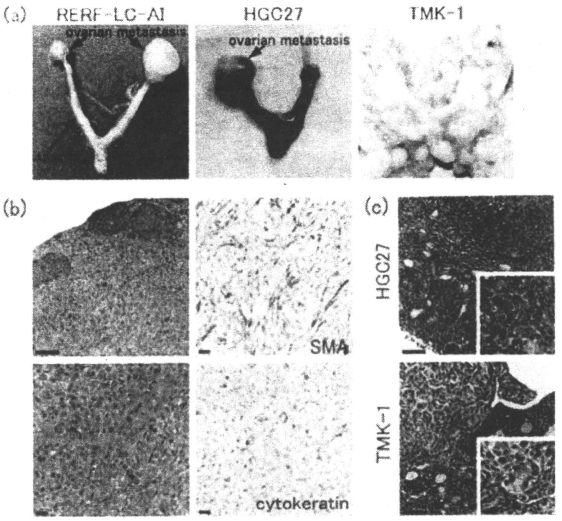

Fig. 1. Experimental metastasis by inoculation of human carcinoma cell lines. (a) Macroscopic findings of mouse ovarian tumors. Transevenous inoculation of RERF-LC-AI and intraperitoneal inoculation (i.p.) of HGC27 caused bilateral and unilateral enlargement of the ovaries, respectively. In the i.p. experiment of TMK-1, the ovaries were entirely buried in the disseminated tumor. (b) Histology and immunohistochemistry (smooth muscle actin [SMA] and human specific cytokeratin) of mouse ovarian tumors of RERF-LC-AI. Bar = 100 μm (left upper), 20 μm (the others). RERF-LC-AI cells diffusely infiltrated the ovary, and there remained only little normal ovarian tissue. In metastatic tissue, stromal reaction of ovarian fibroblasts was observed. (c) Histology of ovarian tumors established by i.p. of HGC27 and TMK-1. Insets show larger magnification of the tumor (HGC27) and the border region of tumor and normal ovarian tissue (TMK-1). HGC27 cells proliferated in the ovary (M), and normal ovarian tissue (N) remained in lower part of the figure, surrounding the metastatic tumor. This finding indicates metastasis to the ovaries, not invasion. With TMK-1, we observed the invasion of cancer cells from the surface of the ovary. Bar = 100 μm, 10 μm (insets).

Table 3. Organ distribution of experimental metastasis after intraperitoneal inoculation of the different cell lines

Cell line	Organ						Days after inoculation
	Ovary (unilateral/bilateral)		Peritoneal dissemination	Ascites	Liver	Lung	
	Metastasis	Invasion					
TMK-1	0/10 (0%)	5/10 (50%) (5/0)	10/10 (100%)	10/10 (100%)	6/10 (60%)	0/10 (0%)	21–24
HGC-27	1/9 (11%) (1/0)	0/9 (0%)	9/9 (100%)	0/9 (0%)	3/9 (33%)	3/9 (33%)	49–72
MKN-45	1/5 (20%) (0/1)	0/5 (0%)	5/5 (100%)	2/5 (40%)	1/5 (20%)	2/5 (40%)	45–86
MKN-28	0/8 (0%)	2/8 (25%) (2/0)	8/8 (100%)	6/8 (75%)	5/8 (63%)	2/8 (25%)	30–45
MKN-74	0/5 (0%)	0/5 (0%)	4/5 (80%)	0/5 (0%)	2/5 (40%)	0/5 (0%)	33–104
KATO-III	1/4 (25%) (1/0)	0/4 (0%)	2/4 (50%)	0/4 (0%)	2/4 (50%)	0/4 (0%)	101–164
HSKTC	0/12 (0%)	0/12 (0%)	1/12 (8%)	0/12 (0%)	0/12 (0%)	0/12 (0%)	119–264
RERF-LC-AI	1/4 (25%) (1/0)	0/4 (0%)	4/4 (100%)	4/4 (100%)	1/4 (25%)	1/4 (25%)	37

as an *in vivo* model of ovarian metastasis. Histologically, three-quarters of the ovarian tumors in this model demonstrated a stromal reaction, mimicking the sarcomatoid proliferation of ovarian fibroblasts in Krukenberg tumor (Fig. 1b).

Because the formation of tumor foci after transvenous inoculation of the examined cell lines was extremely rare, we also inoculated each cell line intraperitoneally. In this experiment, peritoneal dissemination was observed most often in six of the eight cell lines (Table 3). Ovarian involvement was also observed in these six cell lines; however, in the cases of TMK-1 and MKN-28, the ovaries were buried in the disseminated tumors, and the cancer cells were considered to invade the ovaries directly from predominant adjacently disseminated tumors. On the other hand, by inoculation with HGC27, MKN-45, KATO-III, and RERF-LC-AI, significant enlargement of the ovary without adjacent dissemination was observed (Fig. 1a,c). These four cell lines are considered to have some capacity for metastasizing to the ovary, but even in RERF-LC-AI, ovarian metastasis occurred at only a low percentage by intraperitoneal inoculation (i.p.). After i.p. of RERF-LC-AI, mice became moribund and were sacrificed earlier than after transvenous inoculation (37 days *vs* 53–94 days) (Tables 2 and 3). It can be speculated that in i.p. cases, peritoneal dissemination might debilitate mice so rapidly that ovarian metastasis could hardly be observed when they were sacrificed.

HSKTC, a rare cell line derived from Krukenberg tumor,[21] was also used in our examination. Unfortunately, its tumorigenicity was extremely low, even by intraperitoneal inoculation, and we could not evaluate its affinity for the ovary in *in vivo* experiments.

Down-regulation of E-cadherin in ovarian-metastatic carcinoma cell lines. To characterize the four metastatic cell lines, we searched the common features concerning gene expression. Although we examined the expression of some chemokines and their receptors, these molecules were not commonly expressed in the four cell lines. Then we focused on another molecule,

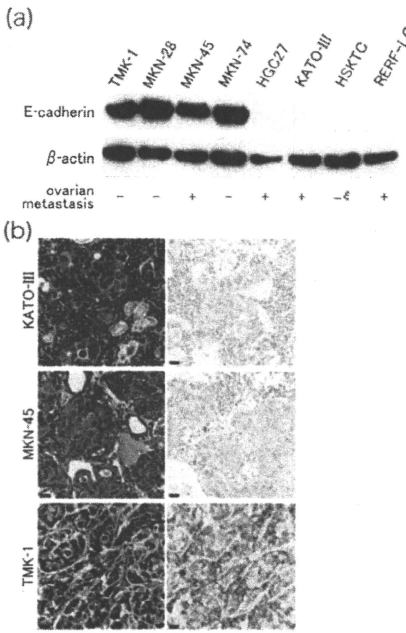

Fig. 2. E-cadherin expression in different carcinoma cell lines. (a) Immunoblot analysis of eight human carcinoma cell lines. Of the four cell lines which clearly metastasized to the ovary, all but MKN-45 demonstrated loss of E-cadherin expression. A Krukenberg tumor cell line, named HSKTC, was also negative for E-cadherin, although it showed extremely poor tumorigenicity in NOD/SCID mice (§). All non-'ovarian-metastatic' cell lines expressed E-cadherin strongly. (b) Hematoxylin–eosin staining and E-cadherin immunohistochemical staining of ovarian lesions of KATOIII and MKN-45, and disseminated tumor of TMK-1. KATO-III was negative for E-cadherin, and MKN-45 showed only weak staining of the cytoplasm. TMK-1 demonstrated positive staining of the cell membranes. Bar = 20 μm.

E-cadherin, whose down-regulation and inactivation in these cells have been reported previously.[23,24] We examined E-cadherin expression of the eight carcinoma cell lines by immunoblot analysis and immunohistochemical staining of mouse tumors. The three of four 'ovarian-metastatic' cell lines and HSKTC showed loss of E-cadherin expression in immunoblot analysis and immunohistochemistry (Fig. 2a,b). Although MKN-45, an 'ovarian-metastatic' cell line, was E-cadherin-positive in immunoblot analysis, its metastatic tumor demonstrated only weak cytoplasmic staining by E-cadherin immunohistochemistry (Fig. 2b). Dysfunctional E-cadherin by an in-frame deletion mutation of the gene in MKN-45 cells[23] seems to be involved in the cytoplasmic localization. On the other hand, non-'ovarian-metastatic' cell lines TMK-1, MKN-28, and MKN-74, were positive on E-cadherin immunoblotting and also showed strong membranous staining in immunohistochemistry.

Inhibition of ovarian metastasis by E-cadherin expression. To investigate whether E-cadherin down-regulation has any effect on ovarian metastasis, the murine E-cadherin gene was transfected into RERF-LC-AI, which showed a high propensity for metastasis to the ovary by transvenous inoculation. Transfectant clones were confirmed to express E-cadherin by immunoblot analysis (Fig. 3a), and immunocytochemistry proved the localization of E-cadherin on cell membranes (Fig. 3b). Three high-expressing clones (LC CDH1-1, -6, -8) and two empty vector-expressing clones (LC vector-3, -4) were inoculated into immune-deficient mice by intravenous injection. None of the E-cadherin transfectants showed tumorigenicity in the ovaries, while mock cells metastasized to the ovaries at high frequency (Table 4). The capacity for metastasis to other organs, such as the pancreas and lung, was maintained in all of the transfectants examined. E-cadherin expression of mouse metastatic tumors of LC CDH1-1, -6, and -8 was confirmed by immunohistochemistry (Fig. 3c). These data indicate that E-cadherin expression specifically inhibited ovarian metastasis in our model.

Classification of clinical ovarian-metastatic tumors by E-cadherin expression. In order to identify whether E-cadherin down-regulation is also observed in clinical cases, we classified 30 cases of ovarian-metastatic tumor by E-cadherin expression examined by immunohistochemistry (Table 5 and Fig. 4). Loss or reduction of E-cadherin expression was observed in 14 cases, and this subset of tumors showed significant associations with a younger population, stomach origin, bilateral involvement of the ovaries, poor differentiation, and stromal proliferation. The other 16 cases demonstrated a strong expression of E-cadherin. Most of these tumors were of colonic origin and well differentiated. Stromal proliferation was rarely observed in E-cadherin-positive cases.

Discussion

Organ-specific metastasis has been investigated intensively and the underlying mechanism has been partly elucidated in several types of carcinoma.[5] The findings of diverse molecules, such as chemokines, growth factors and so on, signal pathways, and new genes have enabled new developments in this field;[1,5] however, there has been no basic research on ovarian-specific metastasis. In the present study, we examined the capacity for metastasis to the ovary in different human carcinoma cell lines. Implantations of the cell lines into NOD/SCID mice were performed

Table 4. Organ distribution of experimental metastasis after transvenous inoculation of RERF-LC-AI transfectants

Transfectant	Organ							Days after inoculation
	Ovary (unilateral/bilateral)	Peritoneal dissemination	Ascites	Pancreas	Liver	Lung	Bone/bone marrow	
LC/CDH1-1	0/5 (0%)	1/5 (20%)	0/5 (0%)	1/5 (20%)	0/5 (0%)	5/5 (100%)	0/5 (0%)	68–163
LC/CDH1-6	0/5 (0%)	3/5 (60%)	0/5 (0%)	0/5 (0%)	0/5 (0%)	3/5 (60%)	0/5 (0%)	70–91
LC/CDH1-8	0/5 (0%)	2/5 (40%)	0/5 (0%)	5/5 (100%)	0/5 (0%)	5/5 (100%)	1/5 (20%)	53–72
LC/vector-3	4/5 (80%) (2/2)	1/5 (20%)	1/5 (20%)	3/5 (60%)	1/5 (20%)	4/5 (80%)	1/5 (20%)	31–66
LC/vector-4	3/4 (75%) (1/2)	4/4 (100%)	2/4 (50%)	3/4 (75%)	1/4 (25%)	4/4 (100%)	0/4 (0%)	66–86

doi: 10.1111/j.1349-7006.2008.00946.x

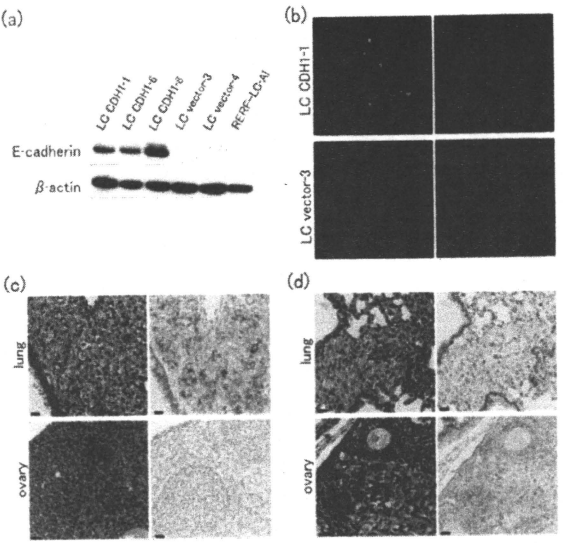

Fig. 3. Expression of E-cadherin in RERF-LC-AI transfectants (a,b) and representative findings of mouse tumors of the transfectants ([c] LC CDH-1 [d] LC vector-3). (a) Immunoblot analysis. E-cadherin transfectants were positive for E-cadherin, while mock clones and the parent cell line were negative. (b) Immunocytochemistry of LC CDH1-1, LC vector-3. Staining of E-cadherin (fluorescein-isothiocyanate–green), filamentous actin (phalloidin-red). LC CDH1-1 cells expressed E-cadherin, and merged staining of E-cadherin, actin, and nucleus (Hoechst-blue) showed membranous colocalization at the cell junction. (c,d) Hematoxylin–eosin staining and E-cadherin immunohistochemistry of the tumors. All clones tested showed tumorigenicity in the lung, and the lung tumors of E-cadherin transfectants showed E-cadherin expression in immunohistochemical staining. None of the E-cadherin transfectants metastasized to the ovary, while the mock clones showed high capacity for ovarian metastasis. Bar = 20 μm.

Table 5. Classification of clinical ovarian metastatic tumors by E-cadherin expression

Variables	E-cadherin expression		*P*-values
	Negative or weakly positive	Positive	
Number of cases	14	16	
Median age	48.6 (29–77)	59.2 (46–78)	0.014*
Primary organ			0.028**
Stomach	10	3	
Colon	2	13	
Breast	1	0	
Unclear	1	0	
Ovarian involvement			0.043*
Bilateral	11	8	
Unilateral	1	7	
Unclear	2	1	
Peritoneal dessemination			0.14
Positive	11	8	
Negative	3	8	
Histological findings of ovarian metastatic tumor			
Differentiation			0.00002**
Well or Moderate	0	12	
Poor	14	4	
Stromal proliferation			0.0002**
Positive	11	2	
Negative	3	14	

*$P < 0.05$; **$P < 0.01$.

transvenously and intraperitoneally. By clinical descriptions,[16,25,26] systemic circulation, peritoneal dissemination, and the lymphatic pathway are thought to be potential anatomical routes for metastasizing to the ovary. In our present model, hematogenous spread as well as the lymphatic pathway may be involved in the ovarian-specific metastasis by both transvenous and intraperitoneal inoculation. Transvenous inoculation of RERF-LC-AI and its transfectants of empty vector caused ovarian metastasis with remarkably high frequency, although the cells also metastasized to the other several organs. It could be considered that there

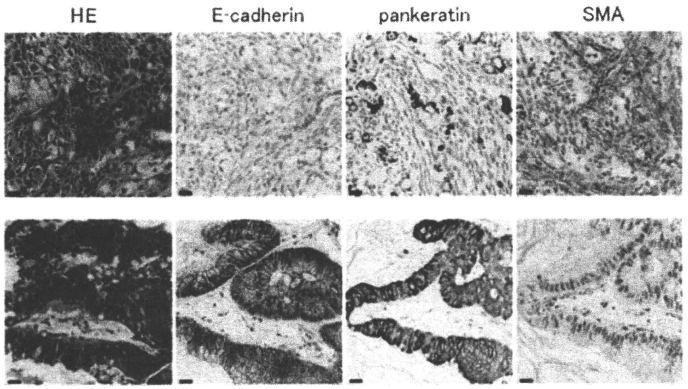

Fig. 4. Representative findings of ovarian metastatic tumors in clinical cases, hematoxylin–eosin (HE) and immunohistochemical staining. E-cadherin-negative or weakly positive case (a) and E-cadherin-positive case (b). HE staining and immunohistochemistry of E-cadherin, pankeratin (AE1/AE3), and smooth muscle actin (SMA). In (a), loss of E-cadherin expression and stromal proliferation were observed. In (b), metastatic tumor of well-differentiated adenocarcinoma showed E-cadherin positivity and relatively poor proliferation of stroma. Bar = 20 μm.

established an *in vivo* model of 'preferential' metastasis to the ovary, and then we utilized this model for investigation of molecular mechanisms of ovarian-specific metastasis.

Because all of the cell lines which metastasized to the ovary by intraperitoneal inoculation showed loss or reduction of E-cadherin expression on immunoblotting and/or immunohistochemistry, we hypothesized that E-cadherin down-regulation might be involved in the mechanism of ovarian-specific metastasis. To examine this hypothesis, RERF-LC-AI was transfected with the murine E-cadherin gene and inoculated into NOD/SCID mice transvenously. Forced expression of E-cadherin in RERF-LC-AI inhibited ovarian metastasis entirely and specifically, as it hardly affected metastasis to the other organs. E-cadherin is a transmembrane glycoprotein localized in the adherens junctions of epithelial cells and acts as a calcium-dependent adhesion molecule.[27] The reduction of E-cadherin expression increases mitotic activity of cancer cells, and promotes invasion and metastasis in general;[28,29] however, the results of our experiments indicate that loss or reduction of E-cadherin expression may promote, in particular, ovarian-specific metastasis. It has been shown that the germ line inactivating mutations in the E-cadherin gene causes hereditary diffuse gastric cancer syndrome, which is characterized by a high risk for diffuse gastric cancer and lobular breast cancer,[30,31] tumors that are associated with increased incidence of ovarian metastasis.[16,32] These data also support the hypothesis that E-cadherin down-regulation might be involved in ovarian-specific metastasis. Because it is hard to explain such involvement by only the function of E-cadherin as an adhesion molecule, there may be other unknown regulatory functions of E-cadherin, which can inhibit metastasis to the ovary.

Especially in organ-specific metastasis, the final step in metastatic events, where circulating cancer cells arrest and form tumor foci at distant sites, is considered to be an essential factor in specificity.[5,6] Those factors depend on the association of the characters of cancer cells and the microenvironment of the distant organ. For instance, osteoblastic bone metastasis of prostate carcinoma is closely associated with a series of biological interactions between tumor cells and bone cells where metastatic tumor cells release growth factors that in turn activate osteoblasts.[7] In classical Krukenberg tumor, ovarian stroma proliferates sarcomatously.[25,26] It can be hypothesized that there may be significant interaction between some types of cancer cells and ovarian stromal cells. Such tumor–stroma interaction may cause unique stromal proliferation and, perhaps as a result, help ovarian-specific metastasis. In our histological examination of clinical ovarian metastatic tumors, loss or reduction of E-cadherin expression was observed in about half of the cases. Interestingly, significant stromal proliferation and E-cadherin down-regulation emerged almost synchronously. Our *in vivo* model also demonstrated both E-cadherin down-regulation in RERF-LC-AI cells and stromal reaction in the ovary. Reduction of E-cadherin may be necessary for possible tumor–stroma interaction in ovarian-metastatic tumors.

In our clinical examination, most primary organs of E-cadherin down-regulated tumors were the stomach or breast, which are anatomically distant from the ovary. On the other hand, the majority of E-cadherin-positive tumors metastasized from the colon, which is relatively close to the ovary. This type of ovarian metastasis is considered to simply depend on anatomical proximity. Therefore, it is speculated that there are multiple types of metastasis to the ovary. The metastasis from relatively distant organs, which could be due to some propensity of cancer cells for ovarian metastasis and be regarded as ovarian-specific metastasis, may require E-cadherin down-regulation. In such type of metastasis, the interaction of carcinoma cells and ovarian stromal cells may help the metastasis.

In conclusion, we established an *in vivo* model of transvenous metastasis to the ovary. Our experiments using this model and investigation of clinical cases suggest the involvement of E-cadherin down-regulation in ovarian-specific metastasis.

Acknowledgments

This research was supported by a grant-in-aid from the 21th Century Center of Excellence (COE) program from the Ministry of Education, Culture, Sports, Science, and Technology of Japan, from the Third Term Comprehensive 10-Year Strategy for Cancer Control from the Ministry of Health, Labor, and Welfare of Japan, and from the Foundation for Promotion of Cancer Research. We are grateful to Tokiko Hirabayashi and Maki Morioka for the excellent technical support.

doi: 10.1111/j.1349-7006.2008.00946.x

References

1 Funasaka T, Raz A. The role of autocrine motility factor in tumor and tumor microenvironment. *Cancer Metast Rev* 2007; **26**: 725–35.
2 Fidler IJ. Critical determinants of metastasis. *Sem Cancer Biol* 2002; **12**: 89–96.
3 Fidler IJ. The organ microenvironment and cancer metastasis. *Differentiation* 2002; **70**: 498–505.
4 Strauli P, Haemmerli G. The role of cancer cell motility in invasion. *Cancer Metast Rev* 1984; **3**: 127–41.
5 Fokas E, Engenhart-Cabillic R, Daniilidis K, Rose F, An H-X. Metastasis: the seed and soil theory gains identity. *Cancer Metast Rev* 2007; **26**: 705–15.
6 Paget S. The distribution of secondary growths in cancer of the breast. *Lancet* 1889; **1**: 571–3.
7 Logothetis CJ, Lin SH. Osteoblasts in prostate cancer metastasis to bone. *Nat Rev Cancer* 2005; **5**: 21–8.
8 Cheng X, Hung MC. Breast cancer brain metastases. *Cancer Metastasis Rev* 2007; **26**: 635–43.
9 Young RH, Schully RE. Metastatic tumors in the ovary: a problem-oriented approach and review of the recent literature. *Semin Diagn Pathol* 1991; **8**: 250–76.
10 Urblight TM, Roth LM, Stehman FB. Secondary ovarian neoplasia: a clinicopathologic study of 35 cases. *Cancer* 1984; **53**: 1164–74.
11 Mazur MT, Hsueh S, Gersell DJ. Metastases to the female genital tract: analysis of 325 cases. *Cancer* 1984; **53**: 1978–84.
12 Fujiwara K, Ohishi Y, Koike H, Sawada S, Moriya T, Kohno I. Clinical implications of metastasis to the ovary. *Gynecol Oncol* 1995; **59**: 124–8.
13 Irving JA, Young RH. Lung carcinoma metastatic to the ovary: a clinicopathologic study of 32 cases emphasizing their morphologic spectrum and problems in differential diagnosis. *Am J Surg Pathol* 2005; **29**: 997–1005.
14 Fitzgibbons PL, Martin SE, Simmons TJ. Malignant melanoma metastatic to the ovary. *Am J Surg Pathol* 1987; **11**: 959–64.
15 Takenoue T, Yamada Y, Miyagawa S, Akiyama Y, Nagawa H. Krukenberg tumor from gastric mucosal carcinoma without lymphatic or venous invasion: report of a case. *Hepatogastroenterology* 2001; **48**: 1211–14.
16 Kakushima N, Kamoshida T, Hirai S *et al.* Early gastric cancer with Krukenberg tumor and review of cases of intramucosal gastric cancers with Krukenberg tumor. *J Gastroenterol* 2003; **38**: 1176–80.
17 Yakushiji M, Tazaki T, Nishimura H, Kato T. Krukenberg tumors of the ovary: a clinicopathologic analysis of 112 cases. *Acta Obst Gynaec Jpn* 1987; **39**: 479–85.
18 Wong PC, Ferenczy A, Fan L, McCaughey E. Krukenberg tumors of the ovary. Ultrastructual, histochemical, and immunohistochemical studies of 15 cases. *Cancer* 1986; **57**: 751–60.
19 Motoyama T, Hojo H, Watanabe H. Comparison of seven cell lines derived from human gastric carcinomas. *Acta Pathol Jpn* 1986; **36**: 65–83.
20 Ochiai A, Tahara E. Growth-promoting effect of gastrin on human gastric carcinoma cell line TMK-1. *Jpn J Cancer Res* 1985; **76**: 1064–71.
21 Ishiwata I, Ishiwata C, Soma M *et al.* Characterization of Krukenberg tumor cell line, especially the biological relationship between cancer and stromal cells. *Exp Pathol* 1990; **38**: 97–108.
22 Shimoyama Y, Hirohashi S, Hirano S *et al.* Cadherin cell-adheion molecules in human epithelial tissues and carcinomas. *Cancer Res* 1989; **49**: 2128–33.
23 Oda T, Kanai Y, Oyama T *et al.* E-cadherin gene mutations in human gastric carcinoma cell lines. *Proc Natl Acad Sci USA* 1994; **91**: 1858–62.
24 Yokozaki H. Molecular characteristic of eight gastric cancer cell lines established in Japan. *Pathol Int* 2000; **50**: 767–77.
25 Bidus MA, Zahn CM, Rose S. Germ cell, stromal, and other ovarian tumors. In: Disia P, Creasman W, eds. *Clinical Gynecologic Oncology*, 7th edn. Philadelphia: Mosby, 2007; 369–95.
26 Kim NK, Kim HK, Park BJ *et al.* Risk factors for ovarian metastasis following curative resection of gastric adenocarcinoma. *Cancer* 1999; **85**: 1490–9.
27 Yoshida-Noro C, Suzuki N, Takeichi M. Mollecular nature of the carcium-dependent cell–cell adhesion system in mouse teratocarcinoma and embryonic cells studied with a monoclonal antibody. *Dev Biol* 1984; **101**: 19–27.
28 Behrens J, Weidner KM, Frixen UH *et al.* The role of E-cadhein and scatter factor in tumor invasion and cell motility. *EXS* 1991; **59**: 109–26.
29 Takeichi M. Cadherins in cancer: implications for invasion and metastasis. *Curr Opin Cell Biol* 1993; **5**: 806–11.
30 Graziano F, Humar B, Guilford P. The role of E-cadherin gene (*CDH1*) in diffuse gastric cancer susceptibility: from the laboratory to clinical practice. *Ann Oncol* 2003; **14**: 1705–13.
31 Pharoah PD, Guilford P, Caldas C. Incidence of gastric cancer and breast cancer in *CDH1* (E-cadherin) mutation carriers from hereditary diffuse gastric cancer families. *Gastroenterology* 2001; **121**: 1348–53.
32 Harris M, Howell A, Chrissohou M, Swindell RI, Hudson M, Sellwood RA. A comparison of the metastatic pattern of infiltrating lobular carcinoma and infiltrating ductal carcinoma of the breast. *Br J Cancer* 1984; **50**: 23–30.